Rapid Communications

Mass distributions of fission fragments from nuclei populated by multinucleon transfer or incomplete fusion channels in ^{6,7}Li + ^{238}U reactions

A. Pal,[1,2,*] S. Santra,[1,2] D. Chattopadhyay,[1,2] A. Kundu,[1,2] A. Jhingan,[3] P. Sugathan,[3] N. Saneesh,[3] Mohit Kumar,[3] N. L. Singh,[4] A. Yadav,[3] C. Yadav,[3] R. Dubey,[3] K. Kapoor,[5] Kavita Rani,[5] Honey Arora,[5] Visakh A. C.,[6] Devinder Kaur,[5] B. K. Nayak,[1,2] A. Saxena,[1,2] S. Kailas,[1] and K.-H. Schmidt[7]

[1]*Nuclear Physics Division, Bhabha Atomic Research Centre, Mumbai 400085, India*
[2]*Homi Bhabha National Institute, Anushaktinagar, Mumbai 400094, India*
[3]*Inter University Accelerator Centre, Aruna Asaf Ali Marg, New Delhi 110067, India*
[4]*Department of Physics, The M.S. University of Baroda, Vadodara 390002, India*
[5]*Department of Physics, Panjab University, Chandigarh 160014, India*
[6]*Department of Physics, Central University of Kerala, Kasaragod, Kerala 671123, India*
[7]*GSI-Helmholtzzentrum für Schwerionenforschung GmbH, D-64291 Darmstadt, Germany*

(Received 21 May 2018; revised manuscript received 17 August 2018; published 24 September 2018)

The multinucleon transfer reaction or incomplete fusion reaction (ICF) is a powerful tool to study fission of exotic nuclei that cannot be formed by stable heavy-ion fusion reactions. In the present work, mass distributions of fission fragments (FFs) from fissioning nuclei ^{241,242,243,244}Pu and ^{240,241}Np populated in multinucleon transfer or ICF reactions on ^{6,7}Li + ^{238}U systems have been studied. Among these, ^{244}Pu, ^{243}Pu, and ^{241}Np are formed by the capture of unstable nuclei ^{6}He, ^{5}He, and t, respectively, by the target ^{238}U. Identification of fissioning nuclei and determination of excitation energies have been performed by finding the details of the outgoing projectile-like fragments detected in coincidence with both the fission fragments on an event-by-event basis. The measurements of FF mass distributions and FF folding angle distributions of different ICF channels confirm that these channels are the prime factors for the modifications in the experimental ratio of asymmetric to symmetric fission yields and the width of folding angle distributions for inclusive fission reported earlier on the same reactions. Comparison among the ratio of asymmetric to symmetric fission yields from ^{241,242,243,244}Pu and ^{240,241}Np nuclei formed in the present reactions, available literature data, and the theoretical calculations using GEF code shows that the shell correction for symmetric fission channels plays an important role in describing the experimental mass distribution.

DOI: 10.1103/PhysRevC.98.031601

The study of transfer or breakup induced fission reactions not only plays an important role in understanding the complete picture of a fission reaction involving a heavy-ion projectile, but is also used to simultaneously obtain a lot of information on the fission of several interesting surrogate reaction channels. Measurements of fission probabilities as a function of excitation energy have been performed using few nucleon transfer or incomplete fusion (ICF) fission reactions, e.g., (d, pf), $(^{3}\mathrm{He}, pf)$, $(^{6}\mathrm{Li}, \alpha f)$, $(^{6}\mathrm{Li}, df)$, etc., to obtain indirect information on neutron induced fission cross sections [1–6]. The multinucleon transfer reaction has been found to be a powerful tool to study the fission of neutron-rich exotic nuclei. In a recent article by Leguillon *et al.* [7], the authors have simultaneously studied the FF mass distributions of several neutron-rich isotopes of Th, Pa, and U, populated by the multinucleon transfer channels in the ^{18}O + ^{232}Th reaction. The role of multichance fission at higher excitation energies has been demonstrated by Hirose *et al.* [8] in order to explain the FF mass distributions of nuclei populated in multinucleon transfer reactions on the ^{18}O + ^{238}U system. Fission experiments taking advantage of transfer or incomplete-fusion reactions are performed not only in direct kinematics [7–11], but also in inverse kinematics [12–14]. To study the effect of transfer fission on anisotropy of inclusive FF angular distributions, Lestone *et al.* [15] measured the transfer induced fission channels in the ^{16}O + ^{232}Th reaction. Though the anisotropies of individual transfer-fission channels are higher than that of total fission, the overall anisotropy that includes the fission events with all possible directions of projectile-like fragments (PLFs) for any particular transfer channel is found to be smaller than total fission, as observed by Pal *et al.* [16] for the ^{6}Li + ^{232}Th system.

The above studies reveal much interesting information on individual transfer-fission channels as well as their effects on total fission. However, very few studies are available on the measurements of FF mass and angular distributions for transfer fissions. Due to the low rate of triple coincidence (of two fission fragments and one PLF), these measurements are in fact challenging.

The apparent enhancement in both the peak-to-valley ratio (P:V) of FF mass distributions and the width of FF folding angle distributions of total fission in reactions involving ^{6,7}Li projectiles at below-barrier energies has been attributed to the

*asimpal@barc.gov.in

 ©2018 American Physical Society

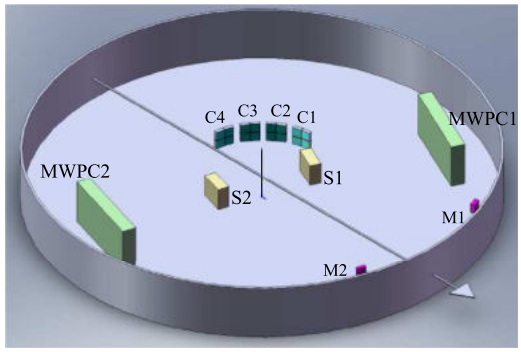

FIG. 1. Schematic diagram of the experimental setup inside scattering chamber.

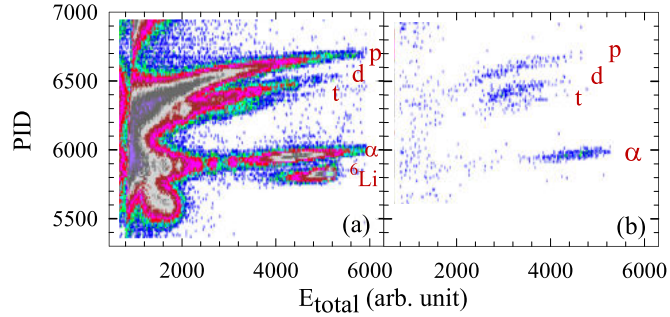

FIG. 2. Typical spectra involving 40 MeV ^{6}Li beam correspond to PID versus energy of a CsI(Tl) detector (a) without any gate and (b) with the gates (see text).

contamination of transfer induced or ICF fission channels in the complete fusion (CF) fission [17,18], where partial energy or different linear momenta are transferred to the composite nuclei. The present work proposes to confirm the above observations by carrying out exclusive measurements on FF mass and angular distributions corresponding to individual transfer or breakup induced fission channels and disentangle their contributions, if possible.

In this Rapid Communication, we present new results on the FF mass and folding angle distributions for transfer or breakup induced fission for ^{6,7}Li + ^{238}U systems measured exclusively at a few energies around the Coulomb barrier. The possible reasons for the unusual behaviors in FF mass and folding angle distributions for the above systems observed previously have been investigated. In addition, the mass distributions of fissioning nuclei ^{241,242,243,244}Pu and ^{240,241}Np populated in multinucleon transfer and/or ICF reactions have been studied.

The experiment on ^{6,7}Li + ^{238}U reactions was carried out at the New Delhi Pelletron facility, using a ^{6}Li beam of 30, 34, and 40 MeV and ^{7}Li beam of 31.4 and 41.4 MeV. The ^{238}U target of thickness ∼100 μg/cm^2 was sandwiched between two layers of ^{12}C of thickness ∼15 μg/cm^2 each. Two multiwire proportional counter (MWPC) detectors [19] were used to detect fission fragments at folding angles. A schematic diagram of the experimental setup is shown in Fig. 1. Each MWPC detector has an active area of 16 × 11 cm^2. The central distances of MWPC1 and MWPC2 from the target center were 39.5 and 33.5 cm, respectively. Each MWPC detector provides position information and a timing signal (STOP signal) for the time-of-flight measurement. The START of the timing signals were taken from two transmission-type gas detectors of active area 3.7 × 3.7 cm^2 (S1 and S2) placed in front of the MWPC detectors at a distance of 11 cm from the target center. Two Si surface barrier detectors (M_1 and M_2) were used as monitors. After position and timing calibrations, the values of the scattering angle θ, azimuthal angle ϕ, and the velocity v of the fission fragments were obtained on an event-by-event basis. Energy loss in the start detector was calculated using the semiempirical formula given in Ref. [20] and the change in velocity due to the energy loss was corrected for each event iteratively until the correct mass of the fission fragment was determined.

Four CsI(Tl) detectors having four crystals each [21] were used to detect the PLFs covering the angular range of 101°–168° for beam energies of 30, 31.4, and 34 MeV and 71°–138° for 40 and 41.4 MeV. The energy spectra of these detectors were calibrated using the known energies of α from a standard ^{229}Th source. A typical "PID (particle identification) versus energy" spectrum obtained from one of the CsI(Tl) detectors for ^{6}Li + ^{238}U reaction at E_{beam} = 40 MeV is shown in Fig. 2(a). The correlation between the time-of-flight signals, $T1$ versus $T2$, obtained from two MWPC detectors provides a clean spectrum of correlated fission events (not shown here). The PID vs energy spectrum of Fig. 2(a) has been gated with the above fission timing distributions as well as the time to amplitude converter spectrum between fission fragments and the PLFs, and the resultant two-dimensional spectrum is shown in Fig. 2(b). It provides clear distinction between p, d, t, and α bands.

Typical FF folding angle distributions for total fission in the laboratory frame for the ^{7}Li + ^{238}U reaction are shown in Fig. 3 for beam energies of (a) 31.4 MeV and (b) 41.4 MeV.

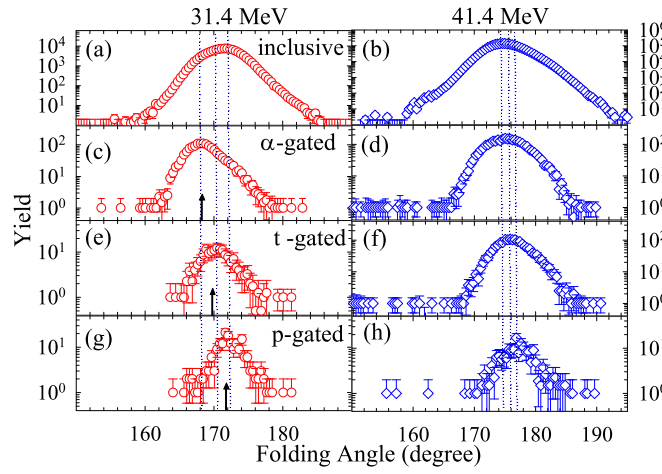

FIG. 3. Typical folding angle distributions for total, α-gated, t-gated, and p-gated fissions in ^{7}Li + ^{238}U reactions at beam energies of 31.4 and 41.4 MeV. Peak positions for α-, t- and p-gated fissions are shown by dotted lines. The up-arrows in the left panels indicate the positions of the folding angles expected from two-body kinematics.

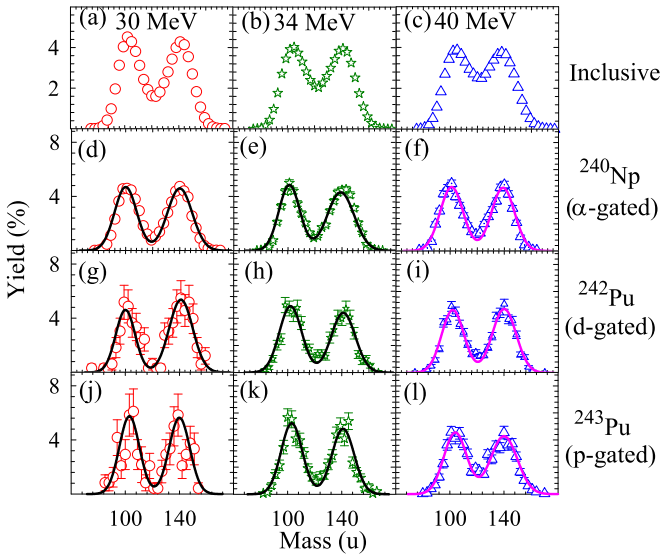

FIG. 4. Mass distribution obtained in ^{6}Li + ^{238}U reactions for total, α-gated, d-gated, and p-gated fissions, at $E_{\rm beam}$ of 30, 34, and 40 MeV.

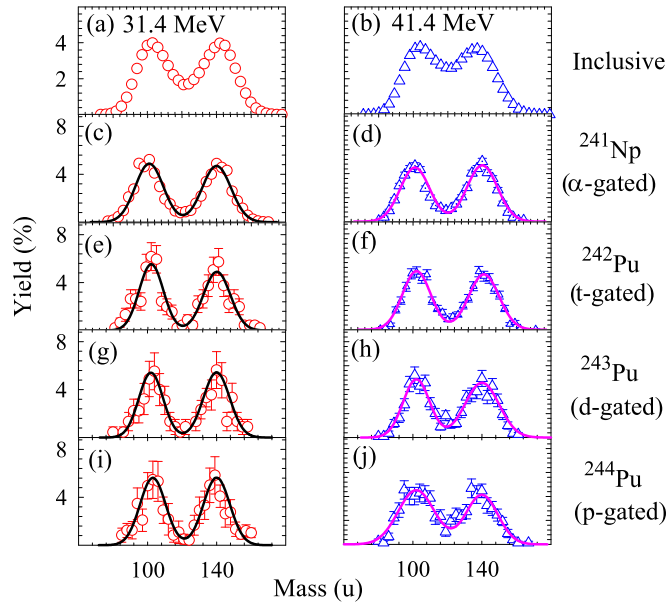

FIG. 5. Same as Fig. 4 but for ^{7}Li + ^{238}U reactions and at $E_{\rm beam}$ 31.4 and 41.4 MeV.

The ones in coincidence with α, t, and p detected in the CsI detector array ($C_1 - C_4$) for the ^{7}Li + ^{238}U reaction are shown in Figs. 3(c)–3(h), respectively, for beam energies of 31.4 and 41.4 MeV. For 31.4 MeV, the peaks in the folding angle distributions of the fission fragments in coincidence with α, t, and p, are observed at ∼168°, 170°, and 172°, respectively (marked by dotted lines), consistent with the kinematics (indicated by up-arrows). The momentum transfer to the target is the highest for α emission at backward angles (grazing angle) for 31.4 MeV, leading to a smaller folding angle for α-gated fission compared to p- or t-gated fissions. The α-gated fission, being the most dominant transfer or ICF channel, is responsible for the presence of the kink at ∼168° (near the main peak at ∼172°) in inclusive FF folding angle distributions at sub-barrier energies. On the other hand, for the 41.4 MeV beam energy, the grazing angle being ∼90°, the mean momentum transfers to the composite nuclei (when proton, triton, and α are PLFs) are similar to that of a CF process leading to a single peak at ∼175° in inclusive FF folding angle distribution.

First, the mass distributions for the inclusive fission events are obtained by assuming all the events to be due to CF fission, i.e., $m_1 + m_2 = m_{\rm CN}$, where m_1 and m_2 are masses of the fission fragments and $m_{\rm CN}$ is that of the compound nucleus. Applying two-body kinematics, the mass distributions obtained (with a mass resolution ∼4–5 u) for inclusive fission in ^{6}Li + ^{238}U and ^{7}Li + ^{238}U reactions are shown in Figs. 4(a)–4(c) and 5(a) and 5(b), respectively. In both reactions, double-humped mass distributions are observed.

The peak-to-valley ratios for the inclusive mass distributions are found to be in good agreement with our earlier measurements [18]. The excitation energy is calculated by $E^* = E_{\rm c.m.} + Q$, with the notation having the usual meaning. As shown in Fig. 6 by red filled circles, the P:V ratio increases with the decreasing excitation energy of the compound nucleus. This is understood in terms of increasing shell effect at lower excitation energies that causes the system to go through asymmetric mass division producing a larger P:V ratio.

Mass distributions for pure CF-fission events are also obtained in the same way as done in Ref. [18], and as expected, the P:V ratio for CF fission, shown as red hollow circles in Fig. 6, are less than the P:V ratio for inclusive fission (red filled circles). To find the contributions from the non-compound fission channels that are producing

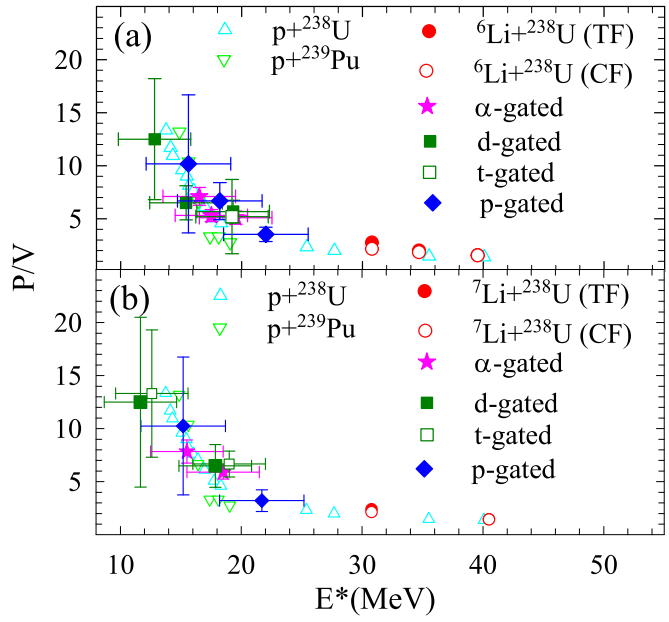

FIG. 6. P:V ratios for total, CF, α-gated, t-gated, d-gated, and p-gated fissions in reactions involving (a) ^{6}Li and (b) ^{7}Li projectiles.

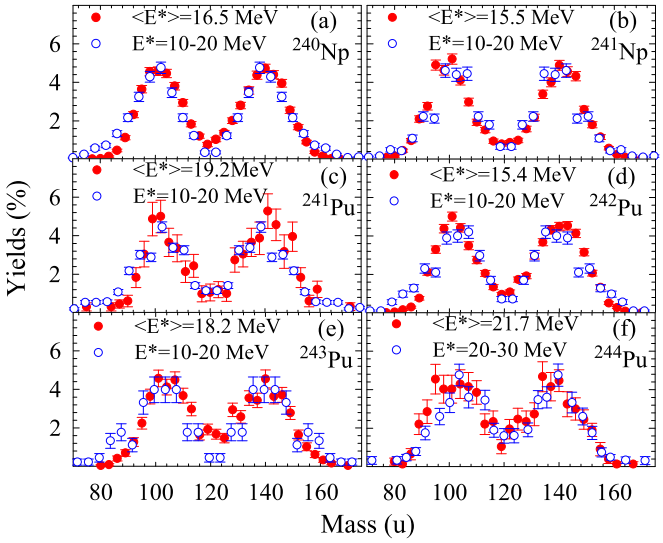

FIG. 7. Comparison of the experimental mass distribution (red filled circles) for ^{240,241}Np and ^{241,242,243,244}Pu nuclei with the literature data (blue hollow circle) [8].

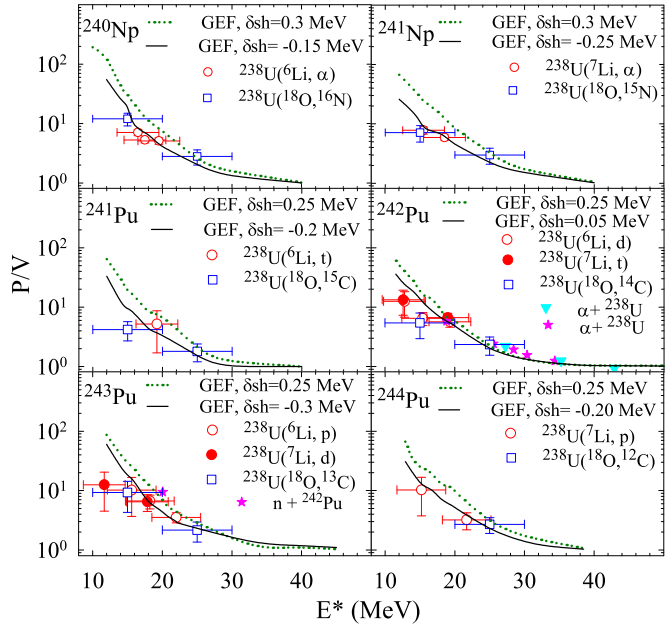

FIG. 8. Comparison of the experimental P:V ratios of nuclei populated in present transfer reactions (circles) with literature data (squares [8], triangles [24], and stars [25,26]) and GEF calculations (solid and dotted lines).

the above discrepancy, the mass distributions for individual ICF- or transfer-fission channels (prime motivation of the present work) are derived separately as follows.

The mass distribution of the fission fragments detected in coincidence with a projectile breakup fragment (say x) is obtained using three-body kinematics with $m_1 + m_2 = m_{\rm CN} - m_x$. For the ^{6}Li + ^{238}U reaction, the fission fragments measured in coincidence with α, t, d, and p are assumed to have been produced from the fission of composite nuclei ^{240}Np, ^{241}Pu, ^{242}Pu, and ^{243}Pu, formed by the capture of the complementary breakup fragments, i.e., d, ^{3}He, α, and ^{5}He, respectively. Similarly, for the ^{7}Li + ^{238}U reaction, the fission fragments measured in coincidence with α, t, d, and p are assumed to have been produced from the composite nuclei ^{241}Np, ^{242}Pu, ^{243}Pu, and ^{244}Pu, formed by the capture of the complementary PLF clusters, i.e., t, α, ^{5}He, and ^{6}He, respectively. However, in the case of p-gated fission for the ^{6}Li(^{7}Li)+^{238}U reaction the complementary breakup fragment is ^{5}He(^{6}He) which is unstable against $n(2n) + \alpha$ breakup and hence only one of the breakup fragments, i.e., α or $n(2n)$ may induce fission. But, the probability of these multistep processes could be considered to be negligible compared to the direct ^{5}He(^{6}He) induced fissions. The mass distributions of fission fragments produced from the composite nuclei ^{244}Pu, formed by the capture of ^{6}He by a ^{238}U target with excitation energy in the range of 15–22 MeV, are measured for the first time in the present work.

The present mass distributions (red filled circles) are compared with the literature data (hollow blue circles) for the same fissioning nuclei at comparable excitation energies in Fig. 7. The center of gravities of heavy and light fragments are around 140–142 u and 100–103 u, respectively, and consistent with Refs. [7,8].

Now, the mass distributions of α-gated fissions are shown in Figs. 4(d)–4(f) and 5(c) and 5(d) for reactions involving ^{6}Li and ^{7}Li projectiles, respectively, corresponding to all the beam energies. It can be observed that for a particular beam energy, the above distributions have more asymmetric mass components compared to those for total fission.

Similarly, the mass distributions of d-gated and p-gated fissions in ^{6}Li + ^{238}U reactions are shown in Figs. 4(g)–4(l), respectively. Due to poor statistics for t-gated fissions involving ^{6}Li beam at lower energies, mass distribution has been obtained only at 40 MeV [Fig. 7(c)]. For the ^{7}Li beam, the mass distributions for fission in coincidence with t, d, and p are shown in Figs. 5(e)–5(j), respectively. The corresponding excitation energies of the composite nuclei are calculated as $E^* = E_{\rm beam} - E_{\rm PLF} - E_{\rm recoil} + Q_{gg}$, with the notations having their usual meanings.

The P:V ratios of the mass distributions of fission fragments gated with α, t, d, and p at respective excitation energies are shown in Fig. 6(a) for ^{6}Li and Fig. 6(b) for ^{7}Li projectiles, respectively. The P:V ratios for all the transfer- or ICF-fission channels are found to be higher than the ones for total fission for a particular beam energy. Obviously, any admixture of ICF fission with CF fission will increase the P:V ratio of the total fission at the excitation energy corresponding to CF fission, thus explaining the difference in the P:V ratios between CF fission and total fission. The measured P:V ratio for each of these transfer induced fissions at proper excitation energy is found to follow the trend of the P:V ratios of mass distributions of fission fragments emitted from similar compound nuclei, populated in p + ^{239}Pu [22] and p + ^{238}U [23] reactions, respectively.

The P:V ratio for all the fissioning nuclei, namely, ^{240,241}Np and ^{241,242,243,244}Pu, are compared with the available literature data as shown in Fig. 8. From the mass distributions reported in Ref. [8], the P:V ratios are deduced and shown as blue

squares in Fig. 8. Additional data for ^{242}Pu [pink stars [25], magenta triangles [24] in Fig. 8(d)] and for ^{243}Pu [pink star [26] in Fig. 8(e)] are also compared. The excitation energy dependence of the present P:V ratio is consistent with the trend of the literature except for the single data point (star) of ^{243}Pu which is lying above the present data (as well as that of Ref. [8]).

The above experimental data are compared with the P:V ratios calculated using a semiempirical code GEF, version 2016/1.2 [27,28], where two main inputs [29] are excitation energy and rms angular momentum. For all the nuclei, the calculations with modified shell correction parameter $\delta_{\rm sh}$ for symmetric fission, represented by black solid lines in Fig. 8, agree with the experimental data (symbols) reasonably well, compared to the calculations with default value (green dotted lines in Fig. 8), implying that the value of the shell correction for symmetric fragments plays an important role in FF mass distribution. The importance of the above shell correction is further illuminated as follows.

In GEF, the P:V ratio of mass distribution depends on the relative yields of the asymmetric and the symmetric fission channels determined by the population of states in the respective fission valleys at or slightly beyond the outer fission barrier in thermal equilibrium. Fission valleys beyond the outer fission barrier are assumed to be essentially formed by fragment shells. In the actinides, where asymmetric fission prevails at low excitation energies, the depth of the asymmetric valley decreases faster than the depth of the symmetric valley as energy increases [30], because the shell effect in the asymmetric valleys is larger.

For asymmetric fission, the nuclear charge of the heavy fragments is almost independent of the fissioning system [31]. The heavy fragment gains $Z \sim 52$ in the standard-1 fission channel and $Z \sim 55$ in standard-2 for all the fissioning systems in the actinide regions due to closed-shell configurations in the heavy fragment. The shell correction for asymmetric fission being large, it is well determined for many fissioning systems and is taken into account in the GEF code (by default). This approach was rather successful in describing the fission-fragment yields of many fissioning systems [28].

In contrast, the mean position (in N and Z) in the symmetric channel unavoidably varies as a function of N and Z of the fissioning system. Since the binding energy of all nuclei in any shape is influenced by shell effects, the depth of the symmetric fission valley is modulated by (normally weak) shell effects. These shell effects depend on the fissioning system, and, thus, the strength of this shell effect in the symmetric valley needs to be fixed by a measured value of the peak-to-valley ratio for the system of interest as done in the present case.

An eventual variation of the (weak) shell effect in the light fragment for different fissioning systems cannot be distinguished and is effectively included in the determined parameter of $\delta_{\rm sh}$.

In summary, the FF folding angle distributions are measured in coincidence with projectile breakup fragments. The peaks of the folding angle distributions corresponding to the dominant transfer- or ICF-fission channels are found to be at same positions where additional kinks are observed in inclusive fission at below-barrier energies. This confirms that the presence of the kinks and the enhancement of the width of FF folding angle distributions at sub-barrier energies is due to the transfer- or ICF-fission channels.

The mass distributions of several nuclei, namely, ^{241,242,243,244}Pu and ^{240,241}Np, populated in multinucleon transfer or ICF channels in the ^{6,7}Li + ^{238}U reactions, are measured for several projectile energies around the Coulomb barrier. The mass distributions of ^{244}Pu nuclei, formed by capture of ^{6}He by the ^{238}U target, are studied in the excitation energy range complementary to that of Ref. [8]. The P:V ratios of mass distributions gated with α, t, d, and p are much larger than the ones for total fission at any particular projectile energy. It provides a direct confirmation that the presence of transfer or ICF fission is the main reason for the enhancement in P:V ratio for inclusive fission compared to CF fission.

Modified value of shell correction for symmetric fission is required in GEF calculations to reproduce the energy dependence of the measured P:V ratio. This observation will initiate more work in both experimental and theoretical realms involving actinide compound nuclei where shell correction for symmetric fragments plays an important role in FF mass distribution.

It is important to note that the mass distributions of the fissioning nuclei ^{244}Pu and ^{241}Np cannot be measured using the fusion reaction of any stable target and stable heavy-ion projectile combination. These nuclei are populated by the capture of ^{6}He and triton, respectively, by the ^{238}U target. Hence, the multinucleon transfer reactions provide us a powerful tool to explore fission studies of nuclei that cannot be populated by stable projectiles.

[1] A. Pal, S. Santra, B. K. Nayak, K. Mahata, V. V. Desai, D. Chattopadhyay, and R. Tripathi, Phys. Rev. C **91**, 054618 (2015).

[2] B. K. Nayak, A. Saxena, D. C. Biswas, E. T. Mirgule, B. V. John, S. Santra, R. P. Vind, R. K. Choudhury, and S. Ganesan, Phys. Rev. C **78**, 061602(R) (2008).

[3] V. V. Desai, B. K. Nayak, A. Saxena, D. C. Biswas, E. T. Mirgule, B. John, S. Santra, Y. K. Gupta, L. S. Danu, G. K. Prajapati *et al.*, Phys. Rev. C **87**, 034604 (2013).

[4] V. V. Desai, B. K. Nayak, A. Saxena, E. T. Mirgule, and S. V. Suryanarayana, Phys. Rev. C **88**, 014613 (2013).

[5] H. C. Britt and J. D. Cramer, Phys. Rev. C **2**, 1758 (1970).

[6] J. E. Escher, J. T. Burke, F. S. Dietrich, N. D. Scielzo, I. J. Thompson, and W. Younes, Rev. Mod. Phys. **84**, 353 (2012).

[7] R. Léguillon, K. Nishio, K. Hirose, H. Maki, I. Nishinaka, R. Orlandia, K. Tsukada, J. Smallcombe, S. Chiba, Y. Aritomod *et al.*, Phys. Lett. B **761**, 125 (2016).

[8] K. Hirose, K. Nishio, S. Tanaka, R. Leguillon, H. Makii, I. Nishinaka, R. Orlandi, K. Tsukada, J. Smallcombe, M. J. Vermeulen *et al.*, Phys. Rev. Lett. **119**, 222501 (2017).

[9] E. Konecny, H. Specht, and J. Weber, Phys. Lett. B **45**, 329 (1973).

[10] K. Nishio, H. Ikezoe, Y. Nagame, S. Mitsuoka, I. Nishinaka, L. Duan, K. Satou, S. Goto, M. Asai, H. Haba *et al.*, Phys. Rev. C **67**, 014604 (2003).
[11] E. K. Hulet, R. W. Lougheed, J. H. Landrum, J. F. Wild, D. C. Hoffman, J. Weber, and J. B. Wilhelmy, Phys. Rev. C **21**, 966 (1980).
[12] M. Caamaño, O. Delaune, F. Farget, X. Derkx, K.-H. Schmidt, L. Audouin, C.-O. Bacri, G. Barreau, J. Benlliure, E. Casarejos *et al.*, Phys. Rev. C **88**, 024605 (2013).
[13] C. Rodríguez-Tajes, F. Farget, X. Derkx, M. Caamaño, O. Delaune, K.-H. Schmidt, E. Clément, A. Dijon, A. Heinz, T. Roger *et al.*, Phys. Rev. C **89**, 024614 (2014).
[14] D. Ramos, M. Caamaño, F. Farget, C. Rodríguez-Tajes, L. Audouin, J. Benlliure, E. Casarejos, E. Clement, D. Cortina, O. Delaune *et al.*, Phys. Rev. C **97**, 054612 (2018).
[15] J. Lestone, J. Leigh, J. Newton, and J. Wei, Nucl. Phys. A **509**, 178 (1990).
[16] A. Pal, S. Santra, D. Chattopadhyay, A. Kundu, K. Ramachandran, R. Tripathi, B. J. Roy, T. N. Nag, Y. Sawant, D. Sarkar *et al.*, Phys. Rev. C **96**, 024603 (2017).
[17] I. Itkis, A. Bogacheva, A. Chizhov, D. Gorodisskiy, M. Itkis, G. Knyazheva, N. Kondratiev, E. Kozulin, L. Krupa, S. Mulgin *et al.*, Phys. Lett. B **640**, 23 (2006).
[18] S. Santra, A. Pal, P. K. Rath, B. K. Nayak, N. L. Singh, D. Chattopadhyay, B. R. Behera, V. Singh, A. Jhingan, P. Sugathan *et al.*, Phys. Rev. C **90**, 064620 (2014).
[19] A. Jhingan, P. Sugathan, K. S. Golda, R. P. Singh, T. Varughese, H. Singh, B. R. Behera, and S. K. Mandal, Rev. Sci. Instrum. **80**, 123502 (2009).
[20] G. Knyazheva, S. Khlebnikov, E. Kozulin, T. Kuzmina, V. Lyapin, M. Mutterer, J. Perkowski, and W. Trzaska, Nucl. Instrum. Methods Phys. Res., Sect. B **248**, 7 (2006).
[21] A. Jhingan, P. Sugathan, G. Kaur, K. Kapoor, N. Saneesh, T. Banerjee, H. Singh, A. Kumar, B. Behera, and B. Nayak, Nucl. Instrum. Methods Phys. Res., Sect. A **786**, 51 (2015).
[22] T. Ohtsuki, Y. Nagame, K. Tsukada, N. Shinohara, S. Baba, K. Hashimoto, I. Nishinaka, K. Sueki, Y. Hatsukawa, K. Hata *et al.*, Phys. Rev. C **44**, 1405 (1991).
[23] R. L. Ferguson, F. Plasil, F. Pleasonton, S. C. Burnett, and H. W. Schmitt, Phys. Rev. C **7**, 2510 (1973).
[24] R. Choudhury, A. Saxena, V. Ramamurthy, D. Nadkarni, and S. Kapoor, Nucl. Phys. A **463**, 597 (1987).
[25] L. Colby, Jr., M. Shoaf, and J. Cobble, Phys. Rev. **121**, 1415 (1961).
[26] I. Winkelmann and D. C. Aumann, Phys. Rev. C **30**, 934 (1984).
[27] B. Jurado and K. H. Schmidt, http://www.khs-erzhausen.de/GEF-2016-1-2.html Computer code GEF, Version 1.2 (2016).
[28] K.-H. Schmidt, B. Jurado, C. Amouroux, and C. Schmitt, Nucl. Data Sheets **131**, 107 (2016).
[29] C. Schmitt, K.-H. Schmidt, and B. Jurado, arXiv:1802.04267.
[30] T. von Egidy and D. Bucurescu, Phys. Rev. C **80**, 054310 (2009).
[31] C. Boeckstiegel, S. Steinhaeuser, K.-H. Schmidt, H.-G. Clerc, A. Grewe, A. Heinz, M. de Jong, A. R. Junghans, J. Mueller, and B. Voss, Nucl. Phys. **A 802**, 12 (2008).